受入
88-4-329
高工研図書室

PHE 87-10

SINGLE DIFFRACTION DISSOCIATION IN π^+p AND K^+p INTERACTIONS AT 250 GeV/c

EHS/NA22 - Collaboration

Aachen - Antwerp/Brussels - Berlin (Zeuthen) - Helsinki -
Krakow - Moscow - Nijmegen - Rio de Janeiro -
Serpukhov - Warsaw - Yerevan

INSTITUT FÜR HOCHENERGIEPHYSIK
AKADEMIE DER WISSENSCHAFTEN DER DDR
BERLIN-ZEUTHEN · DDR

1987

SINGLE DIFFRACTION DISSOCIATION IN π^+p AND K^+p INTERACTIONS AT 250 GeV/c

EHS/NA22 - Collaboration

Aachen - Antwerp/Brussels - Berlin(Zeuthen) - Helsinki - Krakow - Moscow - Nijmegen - Rio de Janeiro - Serpukhov - Warsaw - Yerevan

M.ADAMUS[10], I.V.AJINENKO[9], F.M.L.ALMEIDA Jr.[8], Yu.A.BELOKOPYTOV[9], H.BÖTTCHER[3], P.V.CHLIAPNIKOV[9], F.CRIJNS[7], A.DE ROECK[2a], E.A.DE WOLF[2b], K.DZIUNIKOWSKA[5], A.M.F.ENDLER[8], A.ESKREYS[5], W.FRIEBEL[3], Z.S.GARUTCHAVA[9c], H.GRAESSLER[1], R.S.HACOBYAN[11], P.VAN HAL[7d], T.HAUPT[7e], W.KITTEL[7], A.I.KURNOSENKO[9], S.S.MEGRABYAN[11], F.MEIJERS[7f], A.B.MICHALOWSKA[2], Th.NAUMANN[3], V.I.NIKOLAENKO[9], L.C.S.OLIVEIRA[8], K.OLKIEWICZ[5], E.RIIPINEN[4], H.E.ROLOFF[3], V.M.RONJIN[9], A.M.RYBIN[9], H.M.T.SAARIKKO[4], W.SCHMITZ[1], L.SCHOLTEN[7], N.A.SOTNIKOVA[6], J.STEPANIAK[10], O.G.TCHIKILEV[9], L.A.TIKHONOVA[6], A.G.TOMARADZE[9c], B.A.UTOCHKIN[9], V.A.UVAROV[9], F.VERBEURE[2], R.WISCHNEWSKI[3], S.A.ZOTKIN[6]

Abstract

Results on inclusive single diffraction dissociation in π^+p and K^+p interactions at 250 GeV/c are presented for excited masses up to $\approx$ 9 GeV. Total and topological cross sections for meson and proton diffraction are determined and their energy dependence is studied. For meson diffraction hadronization of the diffractive system is well described by a MC model with $q\bar{q}$-Lund fragmentation and is found to be similar to hadronization in e^+e^- annihilation in terms of thrust and mean charged multiplicity. Fireball-like decay models can be excluded from an elongation of the diffractive meson system along the beam-pomeron axis.

(submitted to Zeitschrift für Physik C)

[1] III.Physikalisches Institut B, RWTH, D-5100 Aachen, Fed.Rep. Germany (partially funded by the German Federal Minister for Research and Technology (BMFT) under the contract number 053AC41P)

[2] Universitaire Instelling Antwerpen, B-2610 Wilrijk and Inter-University Institute for High Energies, VUB/ULB, B-1050 Brussels, Belgium

[3] Institut für Hochenergiephysik der Akademie der Wissenschaften der DDR, DDR-1615 Berlin-Zeuthen, German Dem. Rep.

[4] Department of High Energy Physics, University of Helsinki, SF-00170 Helsinki, Finland

[5] Institute of Physics and Nuclear Techniques of the Academy of Mining and Metallurgy and Institute of Nuclear Physics, PL-30055 Krakow, Poland (partially supported by grants from CPBP 01.06 and 01.09)

[6] Moscow State University, SU-117234 Moscow, USSR

[7] University of Nijmegen and NIKHEF-H, NL-6525 ED Nijmegen, The Netherlands

[8] Centro Brasileiro de Pesquisas Fisicas, 22290 Rio de Janeiro, Brazil

[9] Institute for High Energy Physics,SU-142284 Serpukhov, USSR

[10] University of Warsaw and Institute of Nuclear Problems, PL-00681 Warsaw, Poland (partially supported by grants from CPBP 01.06 and 01.09)

[11] Institute of Physics, SU-375036 Yerevan, USSR

---

[a] Onderzoeker IIKW, Brussels, Belgium

[b] Bevoegdverklaard Navorser NFWO, Belgium

[c] Visitor from Institute of High Energy Physics of Tbilisi State University, USSR

[d] Now with Ericsson Telecommunicatie B.V., Rijen, The Netherlands

[e] On leave from Inst. of Nuclear Physics, Krakow, Poland

[f] Now at CERN, Geneva, Switzerland

1. INTRODUCTION

Diffraction dissociation has attracted new attention due to a dedicated ISR experiment [1] and an experiment [2] in the energy range opened up by the $S\bar{p}pS$ Collider. Both experiments focus on the question, whether the decay of the diffractively excited proton system is isotropic like a fireball or elongated like a fragmentation chain.

The R608 Collaboration [1,3] has studied exclusive diffractive channels. The results are in agreement with the idea of pointlike pomeron-quark coupling [4,5] leading to the back-scattering of one of the proton quarks and a continuing spectator diquark, as in deep-inelastic scattering. The hadronization of the diffractive system is well described by a LUND string [3,6]. The excitation mass M_D, however, is limited to rather low values.

Early results on inclusive proton diffraction at the ISR [7,8] were inconclusive on the question of elongation. However, at collider energies a rapidity plateau develops [2] at the highest diffractive masses ($M_D \approx 140$ GeV) indicating an elongation of the diffractive system. The results can be reproduced by Dual Parton Models (DPM) [9], where chains are stretched between valence constituents of the excited proton and sea constituents of the non-excited one.

So far, the excitation of q(qq) systems in proton diffraction has been considered and compared to lepton-hadron and non-diffractive hadron-hadron collisions. In meson diffraction dissociation a $q\bar{q}$ system should be excited. Such a system is simpler and, according to jet universality [10], can be compared with the cleaner e^+e^- collisions. The disadvantage of the relatively low excitation energy available

at present in meson diffraction is compensated by an increased rapidity range for pions and by the existence of very differential data. In earlier experiments, the dependence of the charge multiplicity on the excitation mass M_D has been studied for $M_D \leq 6$ GeV [11,12] and, indeed, interesting similarities to e^+e^- annihilation have been observed [13].

In this paper, results are presented on single diffraction dissociation of both beam and target in π^+p and K^+p interactions at 250 GeV/c, the highest energy so far reached for positive meson-proton collisions.

The experimental data are discussed in sect.2. In section 3 the method used to isolate the diffractive event samples is described and topological and differential cross sections are given. Results on hadronization properties of the meson diffractive system are presented in sect.4 with emphasis on the question of elongation of the diffractive system. The main results are summarized in sect.5.

2. EXPERIMENTAL DATA

The experiment has been performed at the CERN SPS, in the European Hybrid Spectrometer (EHS) equipped with the Rapid Cycling Bubble Chamber (RCBC) as active vertex detector and exposed to a tagged meson enriched beam of 250 GeV/c. Details on the beam, the experimental set-up, and the interaction trigger used are described elsewhere [14,15]. The EHS offers a 4π acceptance for charged particles and a good momentum resolution ranging from a maximum $\langle \Delta p/p \rangle$ of 2.5 % at 30 GeV/c to 1.5 % above 100 GeV/c.

For the present study, events are accepted when measured and reconstructed multiplicity are consistent, charge balance

is satisfied and all tracks including the beam satisfy certain quality criteria (e.g. $\Delta p/p < 0.25$, track residuals $\sigma < 500$ μm). Events are excluded as elastic if they give a kinematic fit to the elastic hypothesis or simultaneously fulfil conditions in missing transverse momentum ($\Delta p_T < 100$ MeV/c), missing longitudinal momentum ($|\Delta p_L| < 9.0$ GeV/c), missing mass (MM < 200 MeV) and scattering angle of the fast track (less than 4 mrad). A residual elastic contamination is removed by additional cuts (see sect.3.1.). Our results on elastic scattering are given in ref. [16]. The final sample of inelastic events consists of 17275 π^+p and 19929 K$^+$p interactions representing a sensitivity of 0.8 and 1.1 events/μb, respectively. This corresponds to 30 % of our final π^+p and 100 % of our K$^+$p statistics.

Identification of slow protons ($p_{lab} < 1.2$ GeV/c) is done by a special ionization scan (for 60 % (15 %) of the π^+ (K$^+$) sample) or from mass dependent fits in GEOHYB [15]. Weights have been introduced to account for proton losses due to identification. Events with very slow protons are undetectable in RCBC. Their loss ($\approx$ 3 %) is determined from an exponential extrapolation of the four-momentum transfer distributions. The resulting average proton weight is 1.09. The mass of the beam particle was assigned to the fastest track with positive charge and $p_{lab} > 120$ GeV/c. All other tracks are interpreted as pions.

Each event is weighted to correct for losses induced by the interaction trigger [14]. These depend strongly on the spatial characteristics of the event. The trigger weight is determined for each reconstructed event by extrapolating the outgoing tracks to the trigger elements and by using the

azimuthal symmetry around the beam axis, to calculate the fraction of events vetoed by the trigger. The method has been checked by tracking Monte Carlo (MC)-generated events [15]. The average trigger weights for 2-, 4- and 6-prongs are 1.5, 1.2, 1.02 in the beam- and 1.9, 1.8 and 1.6 in the target diffraction sample.

All results given are obtained after correction for proton identification and trigger efficiencies and after normalization of the accepted events according to the topological cross sections measured by this experiment [14]. In Figs.1 and 2 and tables 1 and 2 we, however, omit the normalization in order to give the "observed" numbers of events.

3. CROSS SECTIONS

3.1. Topological and total cross sections

The extraction of the diffractive signal has been achieved by rather different methods in various experiments. The EHS-spectrometer with its excellent acceptance and momentum resolution allows to analyze the quasi-elastic signals in the Feynman-x distributions of the forward and backward leading particles. From these signals we will derive inclusive diffractive cross sections (as done e.g. in ref.[17,18]) and isolate beam- and target-diffractive event samples, for which hadronization properties will then be studied.

We consider beam diffraction

$$\pi^+ p \longrightarrow \pi^+_D p \qquad (1a)$$

$$K^+ p \longrightarrow K^+_D p \qquad (1b)$$

as well as target diffraction

$$\pi^+ p \longrightarrow \pi^+ p_D \qquad (2a)$$

$$K^+ p \longrightarrow K^+ p_D \ , \qquad (2b)$$

where π^+_D, K^+_D and p_D denote the excited meson or proton system of mass M_D. According to the coherence condition [19] the diffractive mass M_D is restricted to $M_D^2/s \lesssim 0.15$ and, hence, the Feynman-x of the recoiling particle to $/x_F/ \approx 1 - M_D^2/s \gtrsim 0.85$.

In Fig.1 we present the x_F-distribution of identified slow protons p_{slow} for reactions (1) with charge multiplicity $n = 2$, 4, 6, 8 and ≥ 10. The x_F-spectrum for the fastest positively charged hadron, h^+_{fast}, in reactions (2) is given in Fig.2. Events with a negative particle being the fastest in the given hemisphere are excluded from Figs.1 and 2.*)

The leading proton and meson signals are clearly visible for $n = 2$, 4 and 6 without any additional cuts (unshaded histograms in Figs.1 and 2). To further suppress the non-

*) For $n = 2$ we additionally require $/x_F/ < 0.95$ for the second particle, to exclude a residual elastic contamination of 6.7 ± 0.7 % and contributions from diffractive decay products to the leading proton or beam particle signal. A correction is applied for resulting small losses in the diffractive signals.

diffractive background the maximum-rapidity-gap (DYMAX-) method is used: the rapidity gap between the leading particle and its nearest charged neighbour is required to be the largest in the event and to be above 2.0. MC studies using Longitudinal Phase Space(LPS)- or fireball-like decay behaviour of the diffractive system have shown that overall more than 97 % of the diffractive events pass the DYMAX-cut and that only in certain regions of phase space the efficiency is lower (e.g. 80% at M_D = 6.4 GeV). A MC model used to correct the selected diffractive event sample for these inefficiencies is described in sect.4.2.

In what follows we apply the DYMAX-cut for multiplicities $n \geq 4$. As can be seen from the hatched histograms in Fig.1 and 2, this leads to a drastic reduction of the non-diffractive background at $/x_F/ < 0.85$, but leaves the leading particle signals almost unchanged. After this cut, we find evidence for a leading signal also for $n = 8$ and even at higher multiplicities.

We interpret the quasi-elastic proton and meson signals in Figs.1 and 2 as originating from beam and target diffraction according to reactions (1) and (2). The non-diffractive background under the leading signal is approximated by a smooth hand-drawn curve extrapolating the x_F-spectra from $/x_F/ < x_F^{cut}$ to $/x_F/ \approx 1.0$ (solid lines in Figs.1 and 2).

The diffractive cross sections are obtained for each multiplicity separately by counting the signal above background in the region $/x_F/ > x_F^{cut}$. As indicated by arrows in Figs.1 and 2, we use $x_F^{cut} = 0.85$ for slow protons, but $x_F^{cut} = 0.80$ for fast π^+ and K^+ to account for the lower

available energy E_A (see sect.4.1.) and minor resolution effects in proton diffraction.

The resulting numbers of diffractive events found and the cross sections obtained after normalization to the topological cross sections [14] are given in tables 1 and 2. The cross sections for $n \geq 10$ are to be considered rough estimates only. The errors quoted include statistical as well as systematic uncertainties.

Systematic effects dominate and originate from the trigger corrections for $n \leq 4$ and from uncertainties in extrapolating the background for $n \geq 6$. Other methods to determine the background, as e.g. extrapolation of measured Δ^{++} or K^o spectra into the corresponding diffractive region [20] or MC-model parametrizations of the background introduce uncertainities of the same order. Explicitly, we have verified that all cross sections stay within the errors when

- the background is parametrized with the DPM-MC model of ref. [21] or
- cuts are applied in variables other than x_F as e.g. proton scattering angle and π^+/K^+ laboratory momentum as done in ref. [22] or
- a hemisphere cut is used as proposed in ref.[18] instead of the DYMAX method (see ref.[23] for details).

To account for the systematic uncertainties we assign rather conservative systematic errors (10 % - 70 % for $n = 4$ to ≥ 10). It should be realized, however, that the background only amounts to 14 % of the total signal, and mainly comes from the high mass region $M_D \geq 5$ GeV (the background level for $M_D < 5$ GeV is only 6 %).

The total single beam diffraction cross section obtained is 1.90 ± 0.20 mb for π^+p and 1.65 ± 0.18 mb for K^+p collisions. For proton diffraction, the value is 1.70 ± 0.18 mb for π^+p and 1.44 ± 0.16 mb for K^+p collisions.

For the analysis described in the following sections, we define the "diffractive event sample" by means of the same cuts as used to calculate the cross sections. To account for the non-diffractive background, each event is weighted by the fraction of the diffractive signal in the corresponding multiplicity and x_F-bin of Figs.1 and 2.

3.2. Differential Cross Sections

Before discussing the total and topological cross sections we first verify the diffractive properties of the event samples selected.

In Fig.3 we present the distribution in the effective mass squared M_D^2 of the diffractive systems. This variable is calculated as the square of the missing mass to the recoiling particle. The low mass region is dominated by events with $n \leq 4$, while the higher multiplicities contribute mainly to the high mass tail. According to the x_F^{cut}-values chosen the tail extends to $M_D^2 = 70$ GeV^2 for meson and to $M_D^2 = 94$ GeV^2 for proton diffraction.

The double differential cross section $d^2\sigma/dtdM_D^2$ is known to follow an exponential in t, the squared four momentum transfer to the recoiling hadron, and to vary as $1/M_D^2$ for masses $M_D^2 \geq 5$ GeV^2 (for a review see [19]). In Fig.4, $d^2\sigma/dtdM_D^2$ is presented for the beam and target diffractive samples at $t = -0.25$ GeV^2 (0.20 GeV^2 slice). As shown by the dashed lines in Fig.4 our data are indeed compatible with a $1/M_D^2$ dependence for diffractive masses $M_D^2 \geq 5$ GeV^2.

Furthermore, the t-dependence of the diffractive cross section at given mass M_D^2 can be well fitted with an exponential $A \cdot \exp(Bt)$. This is demonstrated in Fig.5 for K^+p beam diffraction in three mass intervals. The slope B decreases from $B = 9.5 \pm 0.6$ GeV^{-2} at $M_D^2 < 5$ GeV^2 to $B = 6.4 \pm 0.4$ GeV^{-2} for $M_D^2 > 20$ GeV^2. A similar dependence of the slope on the diffractive mass has previously been observed by other experiments [19].

3.3. Discussion of Total and Topological Cross Sections

The sum of the cross sections for beam and target diffraction is compared to that determined with two other methods in table 3. In the first method we fit the negative binomial (believed to describe non-single-diffractive charge multiplicity distributions) to $n \geq 10$ and subtract the extrapolation to lower n values from our experimental distribution [14] for $n < 10$. In the second method we make use of a model parametrization of topological cross sections suggested by Goulianos [19]. Even though by the first method we may overestimate low multiplicities, the agreement of both the total diffractive cross section and the multiplicity distribution can be regarded quite satisfactory within errors.

A further confirmation of our results comes from the mean charge multiplicity shift due to diffraction to be discussed in sect.4.1.

Diffractive cross sections for different hadrons can be related when assuming factorization of the diffractive vertex [19]. As a consequence of factorization, the cross sections

for the same hadron dissociating on different targets scale as the corresponding elastic cross sections, i.e.

$$\frac{\sigma(p \xrightarrow{K^+} p_D)}{\sigma(p \xrightarrow{\pi^+} p_D)} = \frac{\sigma_{el}(K^+p)}{\sigma_{el}(\pi^+p)} \quad . \qquad (3)$$

From our data, the left hand side of eq. (3) gives 0.85 ± 0.13 in good agreement with 0.84 ± 0.04 [16] for the right hand side.

Comparing our K^+p data with available data at lower energies [20,24] we notice a rise of (0.75 ± 0.25) mb for K^+ and of (0.54 ± 0.20) mb for proton diffraction in the momentum range from 32 to 250 GeV/c. The 2- and 4-prongs contribute with 44 % to this rise in K^+ and with 37 % in proton diffraction. Due to lack of data at lower energies no such comparison can be made for the π^+p data.

To confront our results with single diffraction data for other meson-proton and (anti)proton-proton collisions we present in Fig.6 a compilation of one-vertex-proton-single-diffraction cross sections from $\sqrt{s} \approx 6$ GeV to SpS$\bar{p}$S Collider energies [17-20,24-28]. In this plot the meson M^{+-} induced proton diffractive cross sections $\sigma(p \xrightarrow{M^{+-}} p_D)$ are scaled up to the one-vertex-proton-diffraction cross section $\hat{\sigma}(p \xrightarrow{P} p_D)$ according to the factorization hypothesis by

$$\hat{\sigma}(p \xrightarrow{P} p_D) = \frac{\sigma_{el}(pp)}{\sigma_{el}(M^{+-}p)} \; \sigma(p \xrightarrow{M^{+-}} p_D) \qquad (3a)$$

while the pp data are reduced by a factor of 0.5. For ISR and UA4 the high mass cross sections are chosen ($M_D^2/s < 0.1$) since our data include diffractive contributions from even a

higher M_D^2/s region. The UA5 results at 200 and 900 GeV/c are given only for $M_D^2/s < 0.05$ [27] (according to ISR and UA4 this lower mass cut leads to a reduction of 0.3 - 0.6 mb).

With the caution necessary when comparing cross sections obtained with rather different methods we find our data to be consistent with other data and these with a slight increase of the diffractive cross section in the energy range considered.

4. HADRONIZATION PROPERTIES

4.1. Average charge multiplicities

From tables 1 and 2 the mean charge multiplicities for the diffractive event samples are found to be 4.23 ± 0.54 and 4.22 ± 0.54 for beam and 4.30 ± 0.56 and 4.24 ± 0.56 for target diffraction in π^+p and K^+p, respectively. Calculated from the average charge multiplicities $< n >$ for all inelastic events (including diffraction) [14] the mean non-single-diffractive charge multiplicities $< n_{NSD} >$ are 9.15 ± 0.12 and 9.05 ± 0.15 for π^+p and K^+p collisions at our energy. The shift in the mean multiplicity $\delta\langle n\rangle = < n_{NSD} > - < n >$ is 0.84 ± 0.17 (0.84 ± 0.18) for π^+p (K^+p), in agreement with a value of 0.88 found from the parametrization of the measured s-dependence of $\delta\langle n\rangle$ in ref. [29].

The dependence of the average charge multiplicity $< n_D >$ of the diffractive system, where $n_D = n - 1$, on its mass M_D is shown in Fig.7 a) and b) for meson and proton diffraction, respectively. The errors indicated are statistical only. Systematic uncertainties are approximately half a unit and are mainly due to the non-diffractive background in the large M_D

tail. The mass dependence of $< n_D >$ as measured in our experiment agrees with meson and proton diffraction data at lower energies [11,12]. As already observed at lower energies [12], we find good agreement between proton and meson data, when plotting $< n_D >$ versus the available energy $E_a = M_D - m_{h^+}$, where h^+ refers to π^+, K^+ or p (not shown).

In the following we will restrict ourselves to the diffractive meson system. Since no significant difference is observed for meson diffraction in π^+p and K^+p collisions both samples are combined.

A comparison of hadronization properties of quark-antiquark systems produced in e^+e^- annihilation and in meson diffraction is already suggested in ref. [13]. Assuming jet universality, similarities can be expected. Such a comparison is presented in Fig.8 for the mean charge multiplicity of the hadronic system at energies $M_D = \sqrt{s}$ [30,31]. Contrary to most of the e^+e^- multiplicity compilations we follow the suggestion of ref. [32] and omit the ADONE data [33] ($\sqrt{s}$ = 1.4 to 3.1 GeV) since they include known biases, clearly stated by the authors. Furthermore, many of the mean charge multiplicities quoted by e^+e^- experiments include charged decay products of K^0_S and/or $\Lambda(\bar{\Lambda})$. We correct these e^+e^- data [31] using measured strange particle multiplicities [30,34]. Errors given in Fig.8 are statistical only. Systematic errors are 5 to 15 % and result from those quoted by the experiments and (to a small extent) from the strange particle correction. Satisfactory agreement of diffractive and e^+e^- multiplicities is found in the region of overlap (M_D > 3 GeV). We note, that our $< n_D >$ values seem to extrapolate to the high energy e^+e^- data much smoother than the MARKI data.

4.2. Thrust analysis for the diffractive meson system

While LPS-like elongation of the diffractive proton system has been observed clearly by UA4 [2] such an elongation is still to be shown for diffractively excited meson systems.

To do that we will study hadronization in inclusive meson diffraction in the mass interval $5.0 < M_D < 8.4$ GeV ($\langle M_D \rangle$ = 6.4 GeV) and compare the data with MC predictions for isotropic (fireball) and LPS-type decay of the diffractive system. We generate diffractive events in two steps:

(1) excitation of a diffractive system with mass M_D and squared four-momentum transfer t according to the measured distributions,

(2) hadronization of that system following either the LPS- or the fireball scheme.

In our model LPS-type hadronization is realized for $\pi^+(K^+)$ diffraction as fragmentation of a $u\bar{d}(u\bar{s})$-quark string in the standard LUND framework [35], where the string is parallel to the beam direction in the beam-pomeron rest frame and the leading flavour is chosen at random [23]. For the fireball-like hadronization the same LUND generated final states are taken and the four momenta are recalculated to give isotropic phase space .

A thrust analysis has been performed for the diffractive meson system. The thrust T is calculated in the rest frame of the diffractive system (beam-pomeron rest frame), which is determined from the momentum of the recoiling proton. A neutral component is added [36] to the charged tracks to provide energy-momentum conservation. The "observed" thrust distribution 1/N dN/dT is presented in Fig.9, together with the predictions from the MC models. The MC events are subject

to the same diffractive cuts as the real events (see sect.3.1.). The data are well described by the LPS (LUND)-type diffraction model, whereas fireball-like hadronization is clearly ruled out already at these relatively low diffractive masses.

Consequently, the LUND inspired diffraction model is used to correct the results presented in this section (except Fig.9) for inefficiencies due to the diffractive cuts given in sect.3.1. Using the same model, we correct the measured distributions for unseen neutral particles, as it is done in e^+e^- experiments [37].

In Fig.10 we present the fully corrected thrust distribution for π^+/K^+ diffraction, together with e^+e^- results from PLUTO at $\sqrt{s}$ = 7.7 GeV [37]. The meson diffractive system is at least as elongated along the thrust axis as are the e^+e^- data.

Finally we investigate the orientation of the elongated meson system in terms of the angle θ_T between the thrust axis and the direction of the beam in the beam-pomeron rest frame. In Fig.11, the $\cos\theta_T$ -distribution is shown for two ranges of the diffractive mass M_D. The thrust axis is orientated along the beam direction, whereas it should be uniformly distributed for fireball-like hadronization. This alignment becomes more pronounced with increasing diffractive mass M_D, average values for $\cos\theta_T$ are $0.72 \pm .01$ for $M_D \leq 5$ GeV and 0.89 ± 0.01 for $M_D > 5$ GeV.

These observations lead to the conclusions that shape and mean multiplicity of hadronization in e^+e^- annihilation and diffractively excited meson systems are similar, and that in hadron diffraction the thrust axis is collimated along the beam-pomeron direction.

5. SUMMARY

On the basis of the leading particle x_F-distributions and the maximum rapidity gap method, we have isolated single diffraction dissociation for masses up to $\approx$ 9 GeV in π^+p and K^+p interactions at 250 GeV/c. The main results are:

(i) The total meson single-diffractive cross section is 1.90 $\pm$ 0.20 mb for $\bar{\pi}^+p$ and 1.65 $\pm$ 0.18 mb for K^+p collisions. Proton diffraction contributes 1.70 $\pm$ 0.18 mb and 1.44 $\pm$ 0.16 mb in π^+p and K^+p collisions, respectively.

(ii) Factorization of the diffractive vertex is found to hold at our energy. The proton diffraction cross section is compatible with a slight increase in the energy range from $\sqrt{s} \approx 6$ GeV to $Sp\bar{p}S$ Collider energies.

(iii) The average charge multiplicity for diffractive events is 4.26 $\pm$ 0.78 and 4.23 $\pm$ 0.78 for π^+p and K^+p, resulting in non-single-diffractive multiplicities of 9.15 $\pm$ 0.12 and 9.05 $\pm$ 0.15, respectively.

(iv) For the diffractive meson system at $\langle M_D \rangle = 6.4$ GeV a thrust analysis reveals a longitudinal structure, well described by a MC model with $q\bar{q}$-LUND fragmentation, and a collimation of the thrust axis along the beam-pomeron direction. Isotropic (fireball-like) decay models are excluded in agreement with recent results on proton diffraction at the $Sp\bar{p}S$ Collider. Hadronization of the diffractively excited meson system is similar in terms of thrust and mean charge multiplicity to that in e^+e^- annihilation.

Acknowledgements

It is a pleasure to thank the EHS coordinator L. Montanet and the operating crews and staffs of EHS, SPS and H2 beam, as well as the scanning and processing teams of our laboratories for their invaluable help with this experiment.

References

[1] A.M.Smith et al. (R608), Phys.Lett. B163 (1985) 267

[2] D.Bernard et al. (UA4), Phys.Lett. B166 (1986) 459

[3] A.M.Smith et al. (R608), Phys.Lett. B167 (1986) 248

[4] A.Donnachie and P.V.Landshoff, Nucl.Phys. B244 (1984) 332

[5] E.L.Berger et al., Nucl.Phys. B286 (1987) 704

[6] G.Ingelman and P.Schlein, Phys.Lett. B152 (1985) 256

[7] G.Bellettini, AIP Conf. Proc. No. 15, High Energy Collisions, 1973 (Stony Brook), ed. Ch. Quigg (American Institute of Physics,New York,1973) p 9

[8] M.G.Albrow et al., Phys.Lett. B51 (1974) 424 and Nucl.Phys. B 102 (1976) 275

[9] V.Innocente,A.Capella,A.V.Ramallo and J.Tran Thanh Van, Phys.Lett. B169 (1986) 285; J.Ranft, Z.Phys. C33 (1987) 517

[10] K.Fiałkowski and W.Kittel, Rep.Prog.Phys. 46 (1983) 1283

[11] F.C.Winkelmann et al., Phys.Rev.Lett. 32 (1974) 121

[12] R.L.Cool et al., Phys.Rev.Lett 48 (1982) 1451

[13] S.P.Misra,A.R.Panda and B.K.Parida, Phys.Rev.Lett. 45 (1980) 332

[14] M.Adamus et al. (NA22), Z.Phys. C32 (1986) 475

[15] P.v.Hal, Ph.D. Thesis, Univ.Nijmegen, 1987

[16] M.Adamus et al. (NA22), Phys.Lett. B186 (1987) 223

[17] R.Goettgens et al., Z.Phys. C19 (1983) 283

[18] D.Brick et al., Phys.Rev. D21 (1980) 1726

[19] K.Goulianos, Phys.Rep. 101 (1983) 169

[20] J.Saudraix et al., Z.Phys. C5 (1980) 105

[21] J.Ranft and S.Ritter, Z.Phys. C20 (1983) 347

[22] I.V.Ajinenko et al., Journ.Nucl.Phys. 46 (1986) 818

[23] R.Wischnewski, Ph.D. Thesis, Berlin(Zeuthen),in preparation

[24] E.A. De Wolf et al., Nucl.Phys. B246 (1984) 431

[25] J.C.M.Armitage et al., Nucl.Phys. B194 (1982) 365

[26] D.Bernard et al. (UA4), Phys.Lett. B186 (1987) 227

[27] R.E.Ansorge et al. (UA5), Z.Phys. C33 (1986) 175

[28] A.Wróblewski, Proc. XIVth Int. Symp. on Multiparticle Dynamics, Lake Tahoe, ed. P.Yager, J.F.Gunion, World Scientific Publishing Co., Singapore 1984, p 573 and ref. therein

[29] M.Bardadin-Otwinowska et al., Z.Phys. C18 (1982) 83

[30] W.Bartel et al. (JADE), Z.Phys. C20 (1983) 187
M.Derrick (HRS), ANL-HEP-CP-86-26

[31] J.L.Siegrist et al. (MARK I), Phys.Rev. D26 (1982) 969
B.Niczyporuk et al. (LENA), Z.Phys. C9 (1981) 1
Ch.Berger et al, (PLUTO), Phys.Lett. B95 (1980) 313
M.Althoff et al. (TASSO), Z.Phys. C22 (1984) 307
M.S.Alam et al. (CLEO), Phys.Rev.Lett. 49 (1982) 357
R.Hollebeek (MARK II), Int.Symp.Lepton and Photon Int., Bonn, 1981

[32] K.Fiałkowski, Krakow preprint TPJU 2/1984

[33] C.Bacci et al.(ADONE), Phys.Lett. B86 (1979) 234

[34] M.Althoff et al. (TASSO), Z.Phys. C27 (1985) 27 and ref. therein

[35] T.Sjoestrand, Comp.Phys.Commun. 27 (1982) 243

[36] S.Brandt and H.D.Dahmen, Z.Phys. C1 (1979) 61

[37] Ch.Berger et al. (PLUTO), Z.Phys. C12 (1982) 297

Table 1:

Cross sections σ and numbers of events for Single Beam Diffraction for charge multiplicities n

	$\bar{\pi}^-p$		K^-p	
n	EVENTS	σ , μb	EVENTS	σ , μb
2	778	528 ± 111	942	466 ± 107
4	1015	844 ± 100	1205	708 ± 87
6	421	377 ± 115	530	336 ± 102
8	96	95 ± 48	139	106 ± 54
⩾10	39	59 ± 42	30	34 ± 25
Total		1903 ± 199		1650 ± 182

Table 2:

Cross sections σ and numbers of events for Single Target Diffraction for charge multiplicities n

	$\bar{\pi}^-p$		K^-p	
n	EVENTS	σ , μb	EVENTS	σ , μb
2	662	450 ± 95	863	427 ± 97
4	875	728 ± 87	1029	604 ± 74
6	410	367 ± 112	413	262 ± 80
8	126	124 ± 63	125	95 ± 48
⩾10	20	30 ± 22	44	51 ± 37
Total		1699 ± 183		1439 ± 157

Table 3:

Sum of the beam and target diffractive cross sections obtained by different methods as function of charge multiplicity n, in mb

	$\bar{\pi}^-p$			K^-p		
n	this work	negative binomial	Goul. param.	this work	negative binomial	Goul. param.
2	0.98±0.15	1.10±0.22	0.89	0.89±0.14	1.06±0.23	0,80
4	1.57±0.13	1.90±0.11	1.56	1.31±0.14	1.70±0.12	1.30
6	0.74±0.16	0.75±0.03	0.82	0.60±0.13	0.68±0.02	0.62
8	0.22±0.08	0.12±0.01	0.31	0.20±0.07	0.17±0.01	0.24
⩾10	0.09±0.05	-	0.14	0.09±0.04	-	0.11
total	3.60±0.27	3.87±0.25	3.75	3.09±0.24	3.61±0.26	3.06

Figure captions

Fig. 1: The Feynman-x distribution of slow protons p_{SLOW} in inelastic π^+p (Fig.1a) and K^+p (Fig.1b) interactions at 250 GeV/c, for charge multiplicities n=2 to ⩾10 (shaded area: events after the maximum-rapidity-gap cut; arrows: x_F-cut for selection of diffractive events; lines: estimated background).

Fig. 2: The Feynman-x distribution of the fastest positive hadron h^+_{FAST} in inelastic π^+p (Fig.2a) and K^+p (Fig.2b) interactions at 250 GeV/c, for charge multiplicities n=2 to ⩾10 (shaded area: events after the maximum-rapidity-gap cut; arrows: x_F-cut for selection of diffractive events; lines: estimated background).

Fig. 3: Normalized distribution of the diffractively produced effective mass squared M_D^2, calculated as missing mass squared to the recoiling particle, for inclusive beam and target diffraction, as indicated.

Fig. 4: Double differential cross section $d^2\sigma/dt\,dM_D^2$ for $t = -0.25$ GeV^2 as a function of the effective mass squared M_D^2, for beam and target diffraction. The dashed lines indicate a $1/M_D^2$ behaviour.

Fig. 5: Distribution in the four-momentum-transfer t_{pp} in three intervals of the effective mass squared M_D^2 for K^+-beam diffraction. The full lines represent fits of an exponential $A\cdot\exp(Bt)$ to the data in the regions indicated.

Fig. 6: One-vertex-proton-single-diffractive cross sections $\tilde{\sigma}(p \xrightarrow{p} p_D)$ as a function of the energy $\sqrt{s}$. Meson-proton data are scaled according to the ratio of the elastic cross sections (factorization), pp data are multiplied by 0.5 .

Fig. 7: Average charge multiplicity $\langle n_D\rangle$ of the diffractive meson (Fig.7a) and proton system (Fig.7b) as a function of its mass M_D.

Fig. 8: Average charge multiplicity $\langle n_D\rangle$ of the diffractive meson system as a function of its mass M_D compared to e^+e^- data at $\sqrt{s} = M_D$. K^+p and π^+p data are combined, e^+e^- data are corrected for K^0_S /Λ decays.

Fig 9: Distribution in thrust of the diffractive meson system (K^+p and π^+p data combined) compared to a LUND- and a fireball-like diffractive MC model. Diffractive masses are 5.0 GeV < M_D < 8.4 GeV. No corrections are applied for diffractive cut and unseen neutrals.

Fig.10: Fully corrected thrust distribution of the diffractive meson system (K^+p and π^+p data combined) compared to that of the hadronic system in e^+e^- annihilation at similar energy. Diffractive masses are 5.0 GeV < M_D < 8.4 GeV.

Fig.11: Distribution in cos Θ_T of the meson diffractive system (K^+p and π^+p data combined) in two intervals of the diffractive mass M_D < 5 GeV and M_D > 5 GeV, where Θ_T is the angle between the thrust axis and the beam-pomeron direction in the diffractive rest frame.

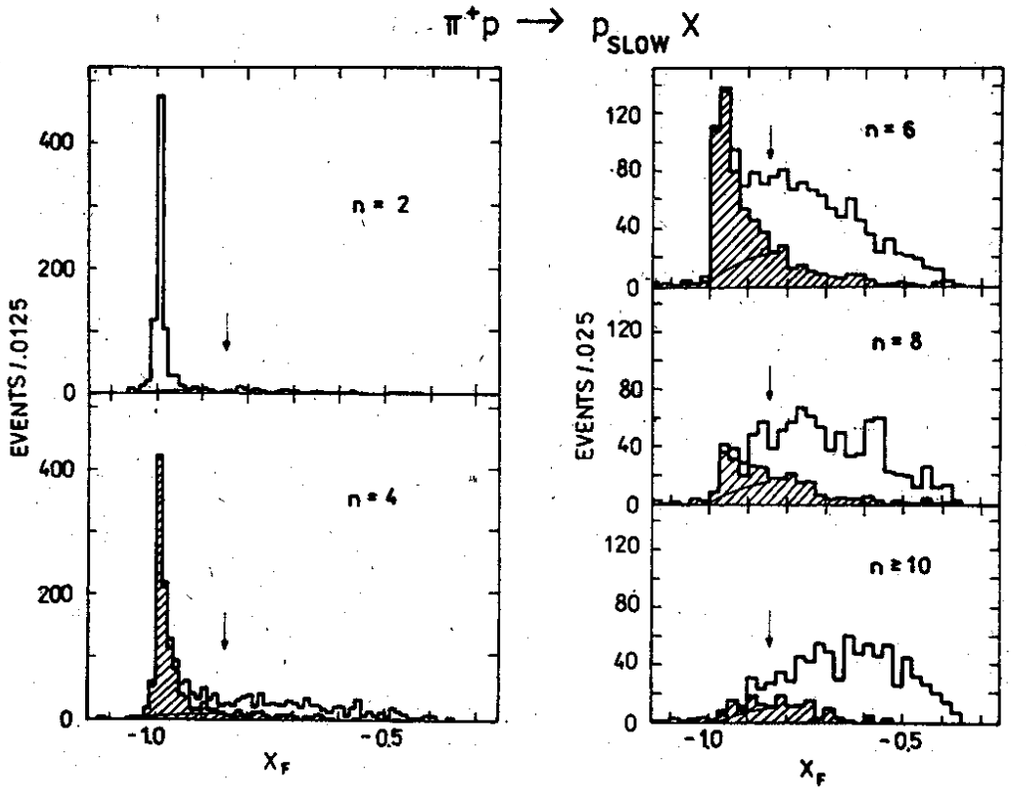
$\pi^+ p \rightarrow p_{SLOW} X$
EVENTS / .0125
EVENTS / .025
n = 2
n = 4
n = 6
n = 8
n ≥ 10
X_F
-1.0
-0.5
0
200
400
40
80
120

FIG. 1a

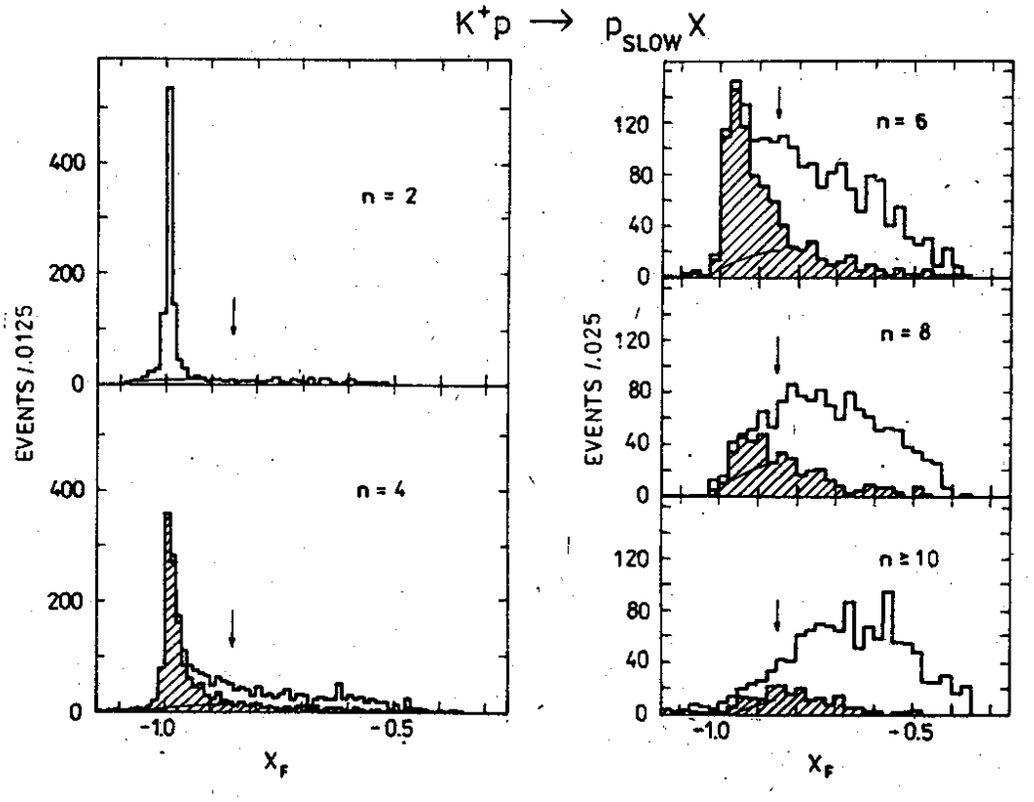
$K^+ p \rightarrow p_{SLOW} X$
EVENTS / .0125
EVENTS / .025
n = 2
n = 4
n = 6
n = 8
n ≥ 10
X_F
-1.0
-0.5
0
200
400
40
80
120

FIG. 1b

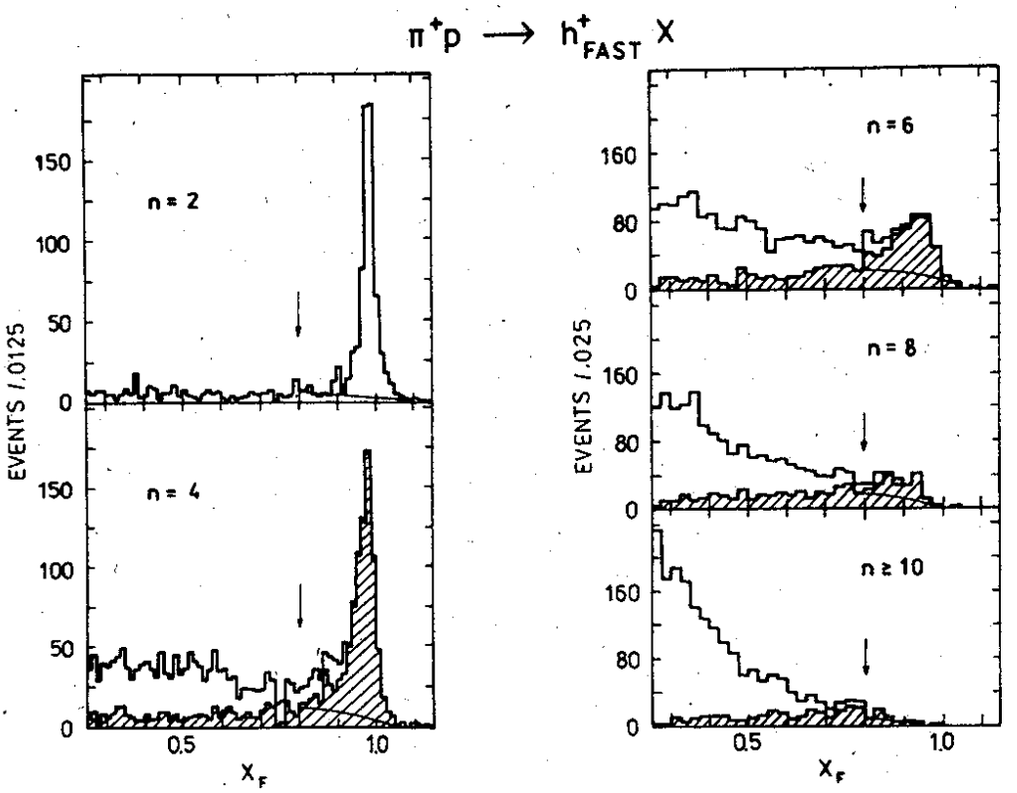
$\pi^+p \longrightarrow h^+_{FAST}\ X$
n = 2
n = 4
n = 6
n = 8
n ≥ 10
EVENTS /.0125
EVENTS /.025
X_F
0.5
1.0

FIG. 2a

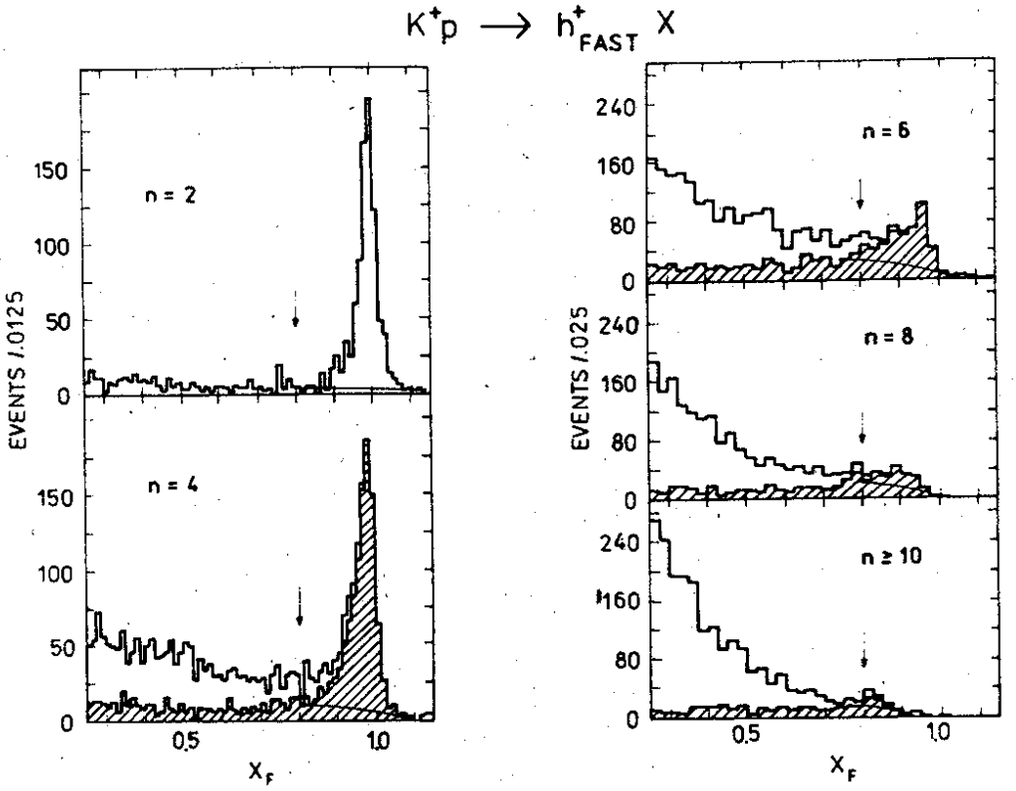
$K^+p \longrightarrow h^+_{FAST}\ X$
n = 2
n = 4
n = 6
n = 8
n ≥ 10
EVENTS /.0125
EVENTS /.025
X_F
0.5
1.0

FIG. 2b

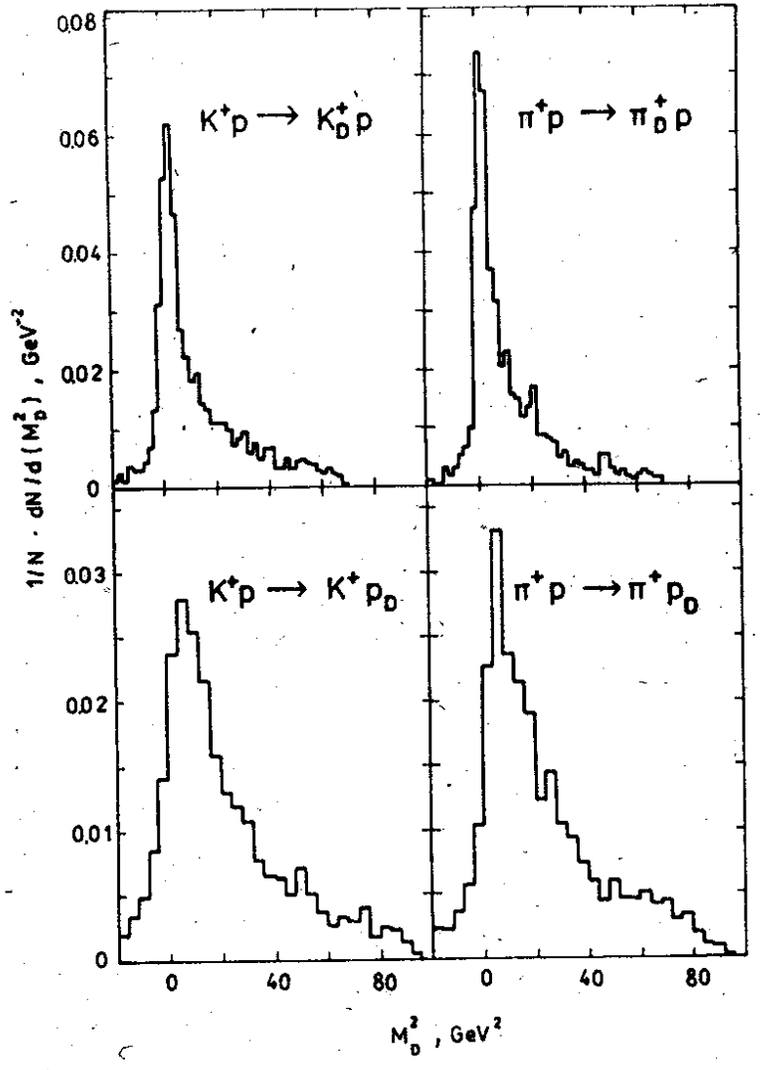
$K^+p \to K^+_D p$
$\pi^+p \to \pi^+_D p$
$K^+p \to K^+p_D$
$\pi^+p \to \pi^+p_D$
$1/N \cdot dN/d(M^2_D)$, GeV^{-2}
M^2_D, GeV^2

Fig. 3

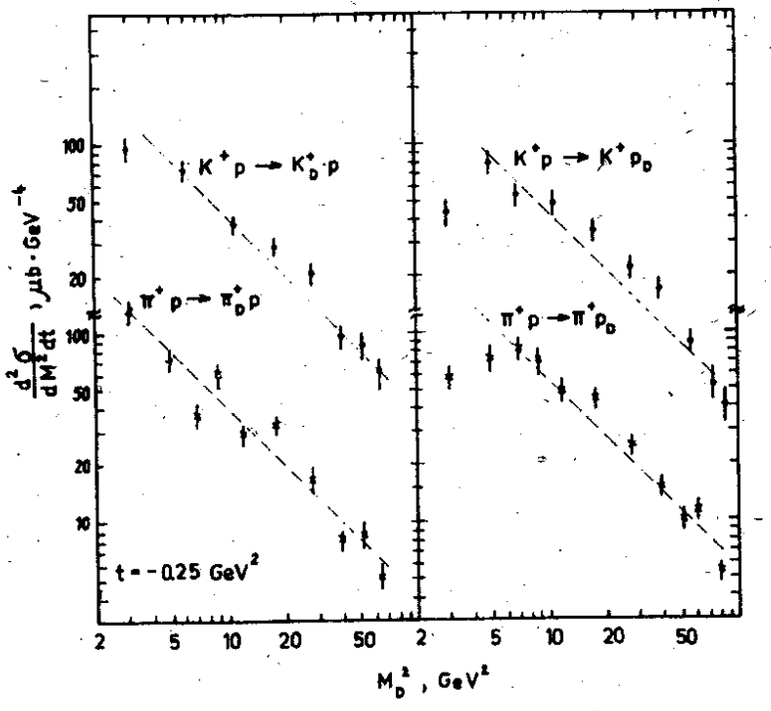
$K^+p \to K^+_D p$
$\pi^+p \to \pi^+_D p$
$K^+p \to K^+p_D$
$\pi^+p \to \pi^+p_D$
$t = -0.25$ GeV^2
$\frac{d^2\sigma}{dM^2dt}$, $\mu b \cdot$ GeV^{-4}
M^2_D, GeV^2

FIG. 4

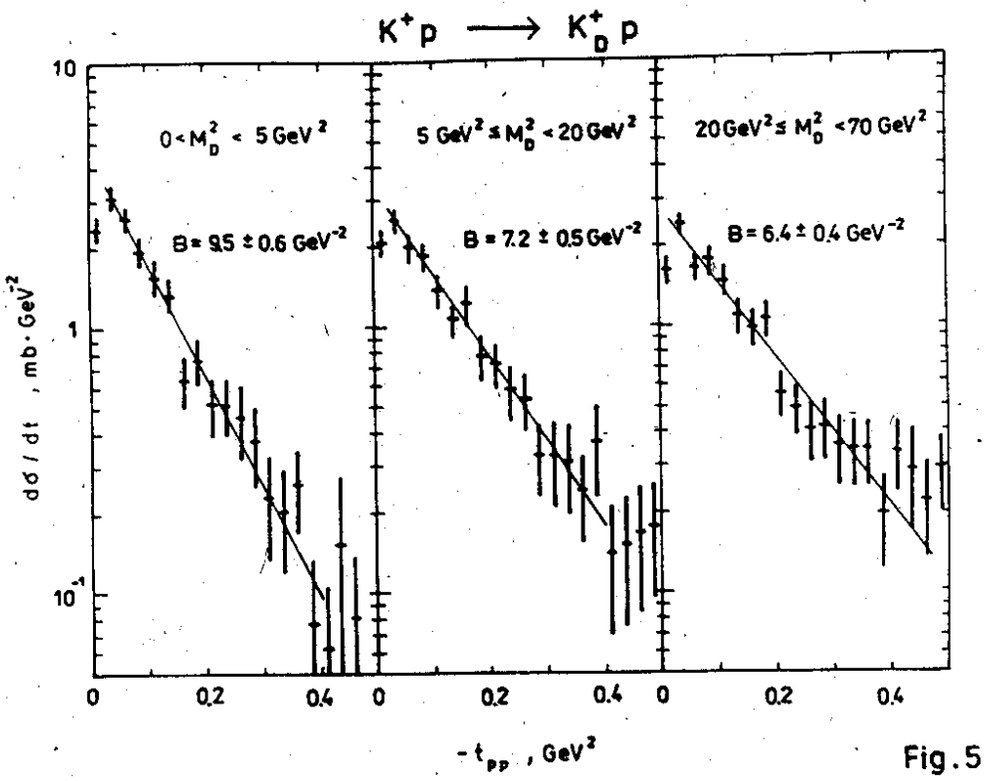
$K^+p \longrightarrow K^+_D p$
$0 < M_D^2 < 5\,GeV^2$
$B = 9.5 \pm 0.6\,GeV^{-2}$
$5\,GeV^2 \le M_D^2 < 20\,GeV^2$
$B = 7.2 \pm 0.5\,GeV^{-2}$
$20\,GeV^2 \le M_D^2 < 70\,GeV^2$
$B = 6.4 \pm 0.4\,GeV^{-2}$
$d\sigma/dt$, $mb \cdot GeV^{-2}$
$-t_{pp}$, GeV^2

Fig.5

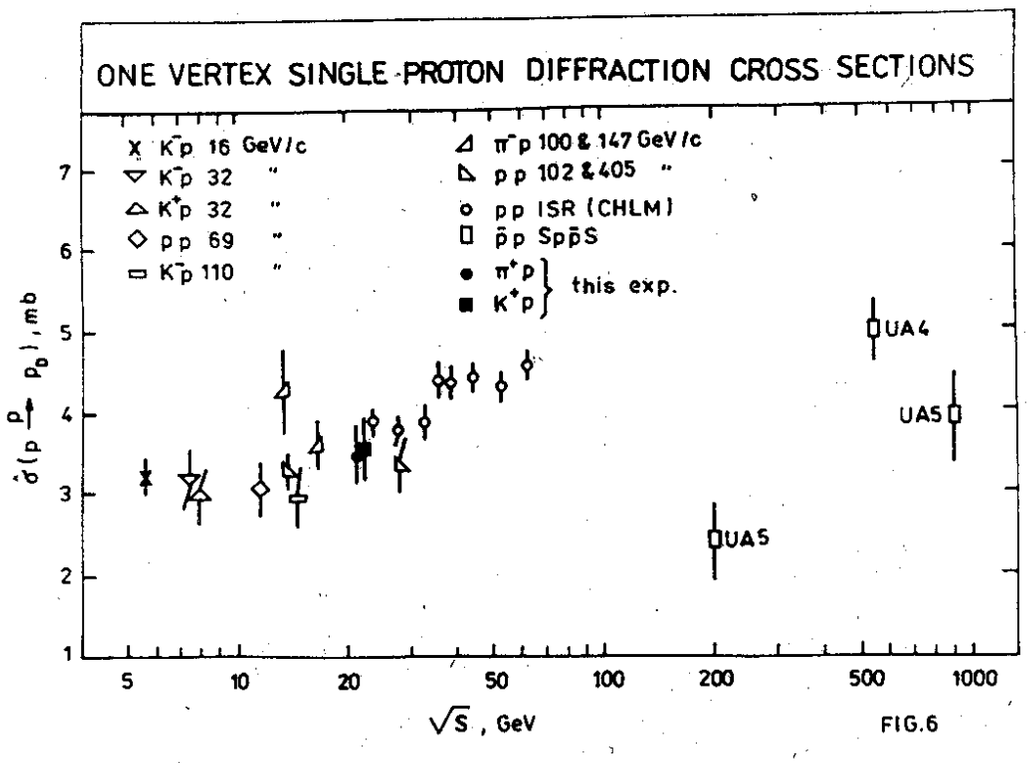
ONE VERTEX SINGLE-PROTON DIFFRACTION CROSS SECTIONS
K^-p 16 GeV/c
K^-p 32 "
K^+p 32 "
pp 69 "
K^-p 110 "
π^-p 100 & 147 GeV/c
pp 102 & 405 "
pp ISR (CHLM)
$\bar{p}p$ SpS
π^+p } this exp.
K^+p }
UA4
UA5
UA5
$\sqrt{s}$, GeV

FIG.6

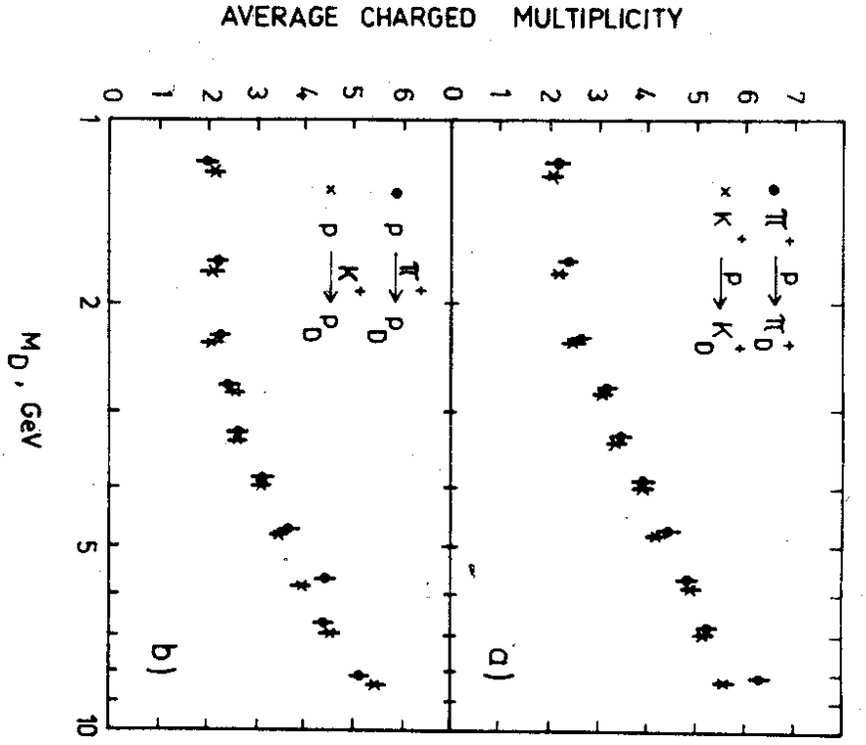
AVERAGE CHARGED MULTIPLICITY
M_D, GeV
b)
a)
$p \to \pi^+_D$
$p \to K^+_D$
$\pi^+ \to p \to \pi^+_D$
$K^+ \to p \to K^+_D$

FIG. 7

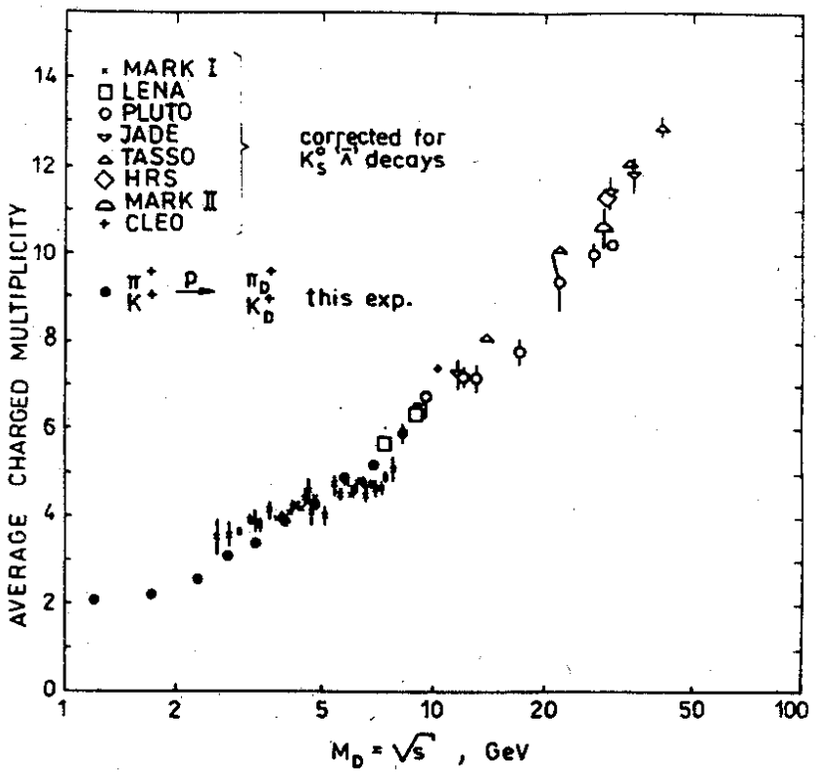
MARK I
LENA
PLUTO
JADE
TASSO
HRS
MARK II
CLEO
corrected for K^0_S (Λ) decays
$\pi^+, K^+ \to p \to \pi^+_D, K^+_D$
this exp.
AVERAGE CHARGED MULTIPLICITY
$M_D = \sqrt{s}$, GeV

FIG. 8

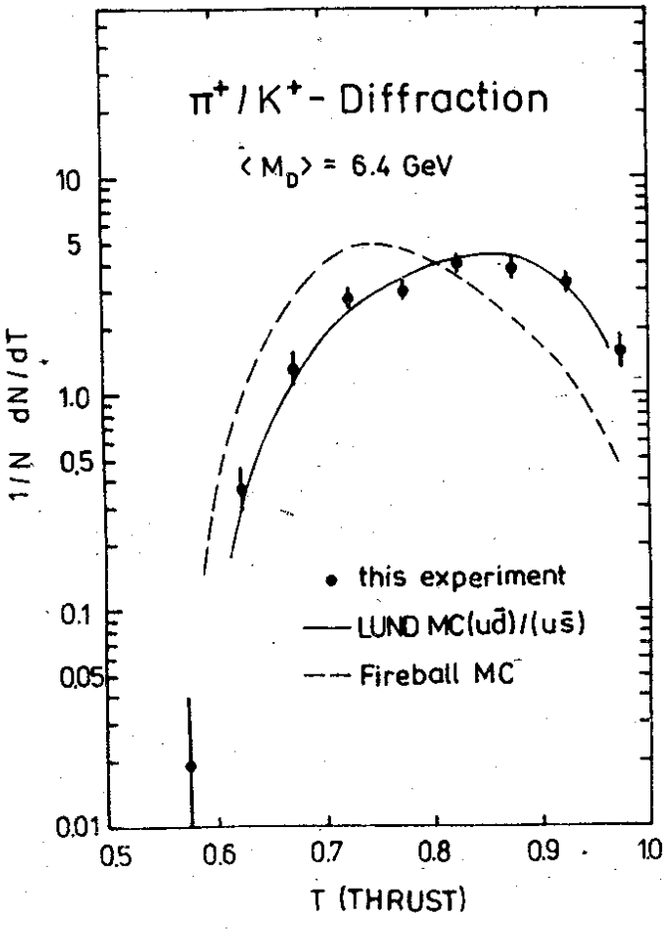
π+ / K+ - Diffraction
⟨ MD ⟩ = 6.4 GeV
1/N dN/dT
10
5
1.0
0.5
0.1
0.05
0.01
0.5
0.6
0.7
0.8
0.9
1.0
T (THRUST)
• this experiment
—— LUND MC(ud̄)/(us̄)
– – – Fireball MC

FIG. 9

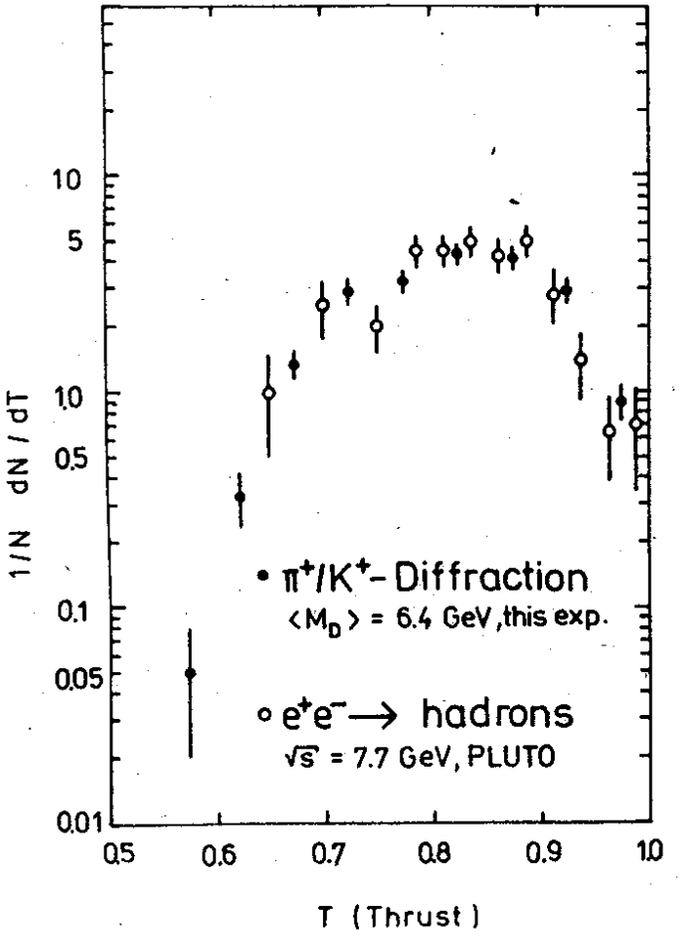
1/N dN/dT
10
5
1.0
0.5
0.1
0.05
0.01
0.5
0.6
0.7
0.8
0.9
1.0
T (Thrust)
• π+/K+- Diffraction
⟨MD⟩ = 6.4 GeV, this exp.
∘ e+e− → hadrons
√s = 7.7 GeV, PLUTO

FIG. 10

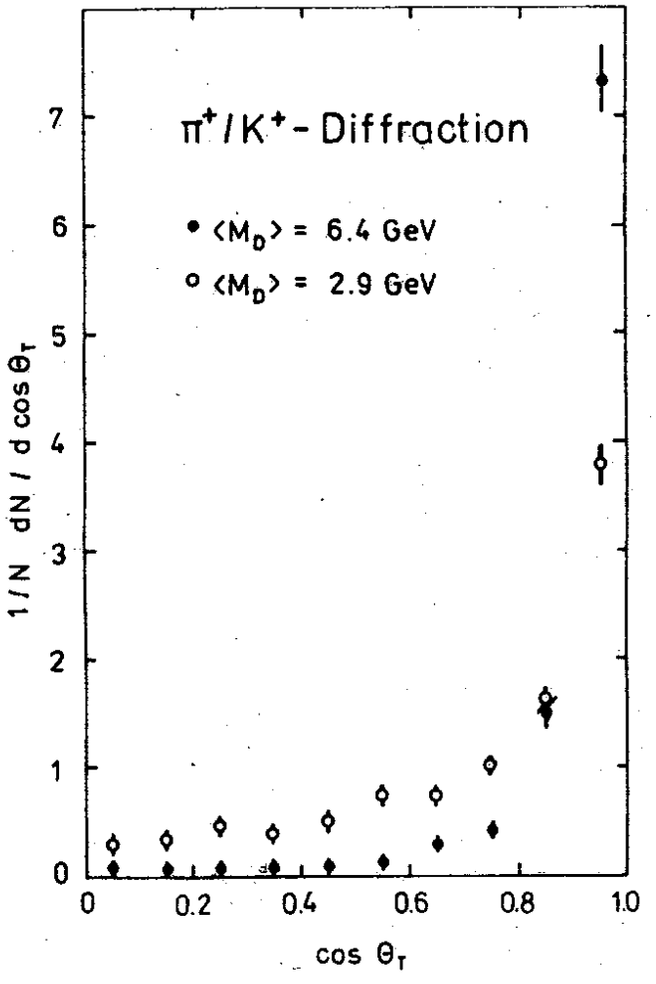
π⁺/K⁺- Diffraction
• ⟨M_D⟩ = 6.4 GeV
○ ⟨M_D⟩ = 2.9 GeV
1/N dN / d cos θ_T
cos θ_T
0
1
2
3
4
5
6
7
0.2
0.4
0.6
0.8
1.0

FIG. 11